The Interferon-Inducible Chemokines MuMig and Crg-2 Exhibit Antiviral Activity In Vivo

SURENDRAN MAHALINGAM,[1] JOSHUA M. FARBER,[2]
AND GUNASEGARAN KARUPIAH[1]*

*Host Defense Laboratory, Viral Engineering and Cytokines Group, Division of Immunology and Cell Biology,
The John Curtin School of Medical Research, The Australian National University, Canberra,
ACT 2601, Australia,[1] and Laboratory of Clinical Investigation, National Institute of
Allergy and Infectious Diseases, National Institutes of Health,
Bethesda, Maryland 20892[2]*

MuMig (murine monokine induced by gamma interferon) and Crg-2 (cytokine responsive gene 2) are two murine chemokines of the CXC family that are induced by the interferons (IFNs): MuMig specifically by IFN-γ and Crg-2 by IFN-α, IFN-β, and IFN-γ. To investigate the biological roles of these chemokines, recombinant vaccinia viruses (rVVs) encoding either MuMig or Crg-2 were constructed. In vitro, the chemokine-encoding rVVs replicated to similar levels to the control virus. Athymic nude mice inoculated with 10^5 PFU or less of VV-HA-Mig or VV-HA–Crg-2 resolved the infection successfully whereas mice given a similar dose of the control virus VV-HA-TK died from generalized infection. At higher doses, there was mortality in all groups but death was significantly delayed in mice infected with either chemokine-encoding rVV compared with those infected with the control virus. Virus-encoded MuMig and Crg-2 enhanced the cytolytic activity of NK cells and splenic cellularity by two- to threefold and resulted in significant increases in mononuclear cell infiltration in the livers of mice. Using specific neutralizing or depleting antibodies, we have established that the control of rVV replication in athymic nude mice, as a consequence of virus-expressed MuMig and Crg-2, requires NK cells and IFN-α, IFN-β, and IFN-γ.

Chemokines are 8- to 12-kDa heparin-binding proteins and have been divided into subfamilies based on the arrangement of conserved cysteine residues: CXC, CC, C and CX$_3$C subfamilies (6). The CXC chemokines can be further subdivided based on the presence of an N-terminal region ELR (glutamic acid-leucine-arginine) sequence, which is important for binding to CXCR1 and CXCR2, the receptors for interleukin-8 (IL-8) and related ELR chemokines on neutrophils. The non-ELR CXC chemokines do not function as neutrophil chemotactic factors. The CC chemokines are chemoattractants for a variety of cells, such as monocytes, lymphocytes, basophils, eosinophils, dendritic cells, and neutrophils (6, 46, 47).

Chemokines are produced as a result of exogenous stimuli, such as viral and bacterial infections, and by endogenous stimuli, such as IL-1, tumor necrosis factor alpha (TNF-α), alpha-beta interferon (IFN-α/β), or IFN-γ. This family of cytokines mediates not only chemotaxis but also leukocyte activation and regulation of leukocyte extravasation from the blood to sites of inflammation. While chemokines have presumably evolved as part of host defense, recent discoveries based on studies of chemokine receptors indicate that microbial pathogens may use the chemokine system to the detriment of the host through molecular piracy (19, 34). Additionally, pathogens as diverse as plasmodia and the immunodeficiency-associated retroviruses use chemokine receptors for entering cells (2, 7, 12–14, 18, 21, 31). Human immunodeficiency virus type 1 (HIV-1) uses the chemokine receptors CXCR4/fusin and CCR5 as coreceptors

with CD4 for membrane fusion and entry (2, 7, 12–14, 18, 31). It is also clear that the CC chemokines RANTES, MIP-1α, MIP-1β and SDF-1 interfere with HIV-1 entry and hence inhibit virus replication. These findings underscore the importance of chemokines and their receptors in the pathogenesis of viral infections.

MuMig (murine monokine induced by gamma interferon) and the murine homologue of IP-10, Crg-2 (cytokine responsive gene 2), are two chemokines identified by differential screening of a cDNA library prepared from lymphokine-activated macrophages (16, 17, 54). Both MuMig and human Mig (HuMig) are inducible by IFN-γ, whereas Crg-2 and IP-10 are inducible by IFN-α/β and IFN-γ (15–17, 54). HuMig and IP-10 have activity as chemotactic factors for NK cells and T lymphocytes in vitro (32, 35, 52, 53). They have the same receptor, CXCR3, which has been found on activated T-lymphocyte clones and cloned NK cells (33). HuMig and IP-10 also cause calcium fluxes in human NK cells (35, 41). It is known that the IFNs mediate antiviral activity through induction of a large number of genes and their encoded proteins. We have shown recently that both the MuMig and Crg-2 genes are prominently induced during experimental infection of mice with vaccinia virus (VV) (3, 36). Together, these findings led us to speculate that MuMig and Crg-2 may, in fact, mediate some of the antiviral effects of IFNs. The critical roles that IFNs play in mediating resistance to VV infection is illustrated by the finding that this virus encodes a number of proteins that can either bind to and inactivate extracellular IFNs or interfere with the intracellular IFN-induced antiviral pathways (1, 51). Furthermore, mice infected with VV can clear the infection in the complete absence of CD8+ cytotoxic T lymphocytes but not in the absence of IFNs (23, 43, 44, 49).

We chose to investigate the activities of MuMig and Crg-2 in host defense against virus by using recombinant VVs (rVVs).

---

* Corresponding author. Present address: Department of Pathology, Blackburn Building, D06, University of Sydney, Sydney, NSW 2006, Australia. Phone: 61 2 9351 2933. Fax: 61 2 9351 3429. E-mail: gunak @medousyd.edu.au.
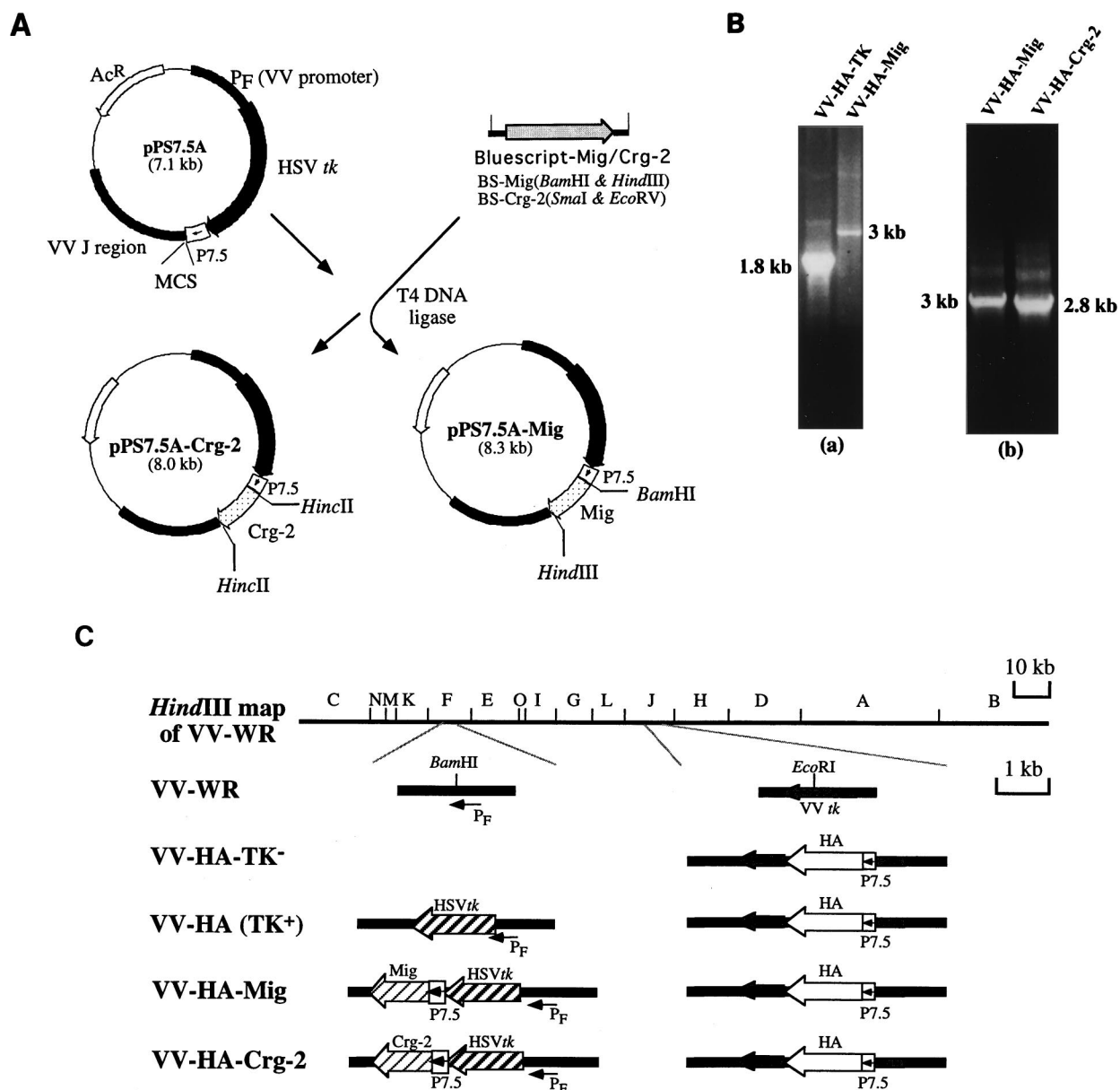
FIG. 1. (A) Construction of insertion plasmids pPS 7.5-Mig and pPS 7.5-Crg-2. The MuMig or Crg-2 fragment was subcloned into vector pPS 7.5A. The gene fragment was inserted in front of a P7.5 promoter in pPS7.5A. (B) PCR of VV DNA. VV DNA was prepared and was amplified by PCR with primers as described in Materials and Methods. DNA from VV-HA-TK yielded a band of 1.8 kb (panel a) while DNA from VV-HA-Mig and VV-HA–Crg-2 yielded bands of 3 and 2.8 kb respectively (panels a and b). Wild-type virus DNA (VV-PR8-HA6) was also amplified. The presence of a wild-type band was not detected in any of the recombinant viruses constructed. (C) Schematic representation of the genomic arrangements of VVs. The HA gene of influenza virus, under the control of the P7.5 promoter, was inserted into the TK gene of vaccinia virus in the HindIII J fragment, yielding VV-HA-TK⁻. The disruption of the TK phenotype was compensated for by insertion of an HSV TK gene in the F fragment under the PF promoter. This gave rise to VV-HA-TK⁺, which was used as the control virus. Marker rescue of VV-HA-TK⁻ with pPS7.5-Mig or pPS7.5–Crg-2 containing HA and Mig or Crg-2 genes produced VV-HA-Mig or VV-HA–Crg-2. PF, VV promoter; P7.5, VV early/late promoter.

Our results demonstrate that MuMig and Crg-2 expressed in vivo at sites of viral replication can produce an antiviral effect and suggest that these chemokines play a role in IFN-mediated defense against viral infection.

MATERIALS AND METHODS

Mice. Female, athymic, Swiss outbred nude mice, 6 to 9 weeks old, bred under specific-pathogen-free conditions, were obtained from the Animal Breeding Establishment, John Curtin School of Medical Research.

Cell lines. YAC-1, a line derived from Moloney murine leukemia virus-induced lymphoma, L929, a murine liver fibroblast cell line, CV-1, a cell line derived from African green monkey kidney, and 143B, a human osteosarcoma cell line, were maintained in Dulbecco's minimal essential medium (Gibco Laboratories, Grand Island, N.Y.) supplemented with antibiotics and 5% heat-inactivated fetal calf serum (FCS; Flow Laboratories, North Ryde, Australia). YAC-1 cells were used as targets in NK cell cytotoxicity assays, CV-1 cells were used for the preparation of virus stocks, L929 and CV-1 cells were used to assess the in vitro growth characteristics of the rVVs, and 143B cells were used for determination of virus titers.

Construction of rVVs. A 1,229-bp fragment containing the MuMig cDNA was excised from pBluescript-SK and cloned into the BamHI and HindIII sites of the digested vector pPS7.5A (10) (Fig. 1A). The 1,008-bp Crg-2 cDNA was cleaved from pBluescript-SK and was then cloned into the HincII site of the digested vector pPS7.5A (Fig. 1A). Expression of both MuMig and Crg-2 are under the

control of the early/late VV 7.5-kDa promoter, P7.5 (obtained from B. Moss, National Institutes of Health, Bethesda, Md.). The resulting plasmids was designated pPS7.5A-Mig and pPS7.5A–Crg-2.

Construction of VV recombinants from the wild-type virus, VV-WR, has been described in detail elsewhere (42). Briefly, Mig- or Crg-2-encoding recombinants VV-HA-Mig and VV-HA–Crg-2 were constructed by the insertion of the herpes simplex virus (HSV) thymidine kinase (TK) gene and a chimeric promoter-Mig or promoter–Crg-2 fragment into the HindIII F region of a VV recombinant, VV-HA-PR8 (4), which had been engineered to express the influenza virus A/PR/8/34 hemagglutinin (HA). The control virus VV-HA-TK, encoding HSV TK and A/PR/8/34 HA but not Mig or Crg-2, was similarly constructed (42). After three rounds of plaque purification, the absence of wild-type virus was confirmed by PCR (Fig. 1B). Viral DNA was extracted as described in detail elsewhere (20). For PCR analysis, 5-μl aliquots of DNA were used. PCR primers FA (5′ GTTTAATATGACGCTCG 3′) and FB (5′ GCGTCACAGAATCT ACC 3′), corresponding, respectively, to the regions 5′ and 3′ from the F-region BamHI site (Fig. 1C), were used to detect the presence of contaminating wild-type virus DNA (the primer sequences were provided by D. Boyle, Commonwealth Scientific and Industrial Research Organization Animal Health Laboratory) by using an FTS thermal sequencer (Corbett Research, Sydney, Australia) and the following conditions: 1 cycle of 94°C for 3 min; 40 cycles of 95°C for 1 s, 50°C for 1 s, and 72°C for 2 min; and 1 cycle of 72°C for 5 min. The genomic configurations of VV-HA-Mig and VV-HA–Crg-2 and the control rVV, VV-HA (10), are shown in Fig. 1C.

Protein expression by recombinant viruses. Chemokine protein expression by the rVVs was determined by Western blot analysis. Briefly, confluent monolayers of CV-1 cells in six-well Linbro cluster plates (Flow Laboratories, McLean, Va.) were infected with VV-HA-Mig or VV-HA–Crg-2 at a multiplicity of infection of 0.1 for 1 h. Unadsorbed virus was removed, and the cells were overlaid with fresh medium containing no FCS. The protease inhibitors leupeptin (2 μg/ml), EDTA (1 mM), and aprotinin (2 μg/ml) (Boehringer Mannheim Biochemicals, Indianapolis, Ind.) were added to the cell culture supernatants before the samples were concentrated in Centricon concentrators (Amicon, Inc., Beverly, Mass.) for analysis. The samples were analyzed on a Tris-glycine-sodium dodecyl sulfate (SDS)–15% polyacrylamide gel by the method of Laemmli (30). Immunoblotting was performed as previously described (32). The proteins were electrotransferred to nitrocellulose membranes (Schleicher & Schuell, Inc., Keene, N.H.) in a TransBlot apparatus (Bio-Rad Laboratories, Hercules, Calif.) at 45 V for 7 h at 4°C. Blots were incubated with rabbit anti-MuMig or rabbit anti-Crg-2 serum at a 1:1,000 dilution, washed with TBS (Tris-buffered saline) and TBS-Tween (TBS plus 0.05% Tween) buffers, and incubated with horseradish peroxidase-conjugated goat anti-rabbit immunoglobulin G (IgG) (Jackson ImmunoResearch Laboratories, Inc., West Grove, Pa.) at a 1:10,000 dilution. The blots were washed again before visualization by chemiluminescence with the ECL reagents as specified by the manufacturer (Amersham Corp., Arlington Heights, Ill.).

In vitro replication of rVVs. CV-1 and L929 cells were seeded (3×10^5 cells/well) in wells of 24-well Linbro cluster plates in Eagle's minimal essential medium Gibco) supplemented with antibiotics and 5% heat-inactivated FCS. After 24 h, cell monolayers were infected with each of the rVVs at a multiplicity of infection of 0.01. The cells were then scraped into the medium, and the contents of each well was harvested at 12, 24, 36, and 48 h postinfection p.i. After three freeze-thaw cycles to release cell-associated virus, a 100-μl volume of each sample was incubated with trypsin as described below for determination of virus titers.

RNA isolation and RT-PCR analysis. Total RNA was isolated from the ovaries, spleens, and cultured splenocytes of the mice by standard methods with RNAzol B (Biotech Laboratories, Houston, Tex.). A reverse transcriptase PCR (RT-PCR) procedure was performed as previously described (51) with some modifications (39). All primers were synthesized at the Biomolecular Research Facility, John Curtin School of Medical Research. Primer and probe sequences for hypoxanthine phosphoribosyltransferase (HPRT) have been described previously (50), while those for MuMig, Crg-2, IFN-α1, IFN-β and IFN-γ are as follows: MuMig, GATCAAACCTGCCTAGATCC (sense), GGCTGTGTAGA ACACAG-AGT (antisense), CTCTTATGTAGTCTTCCTTGAACGACGACG (probe); Crg-2, CGCGGATCCTGAGCAGAGATGTCTGAATC (sense), CGC GGATCCTCGCACCTCCACATAGCTTACAG (antisense), ATTAGGACTA GCCATCCACTGGGTAAAGGG (probe); IFN-α1, TGTCTGATGCAGCAG GTGG (sense), AAGACAGGGCTTCTCCAGAC (antisense), CAGGAATTT CCCCTGACC (probe); IFN-β, CCATCCAAGAGATGCTCCAG (sense), GTGGAGAGCAGTTGAGGACA (antisense), GTACGTCTCCTGGATGA ACT (probe); and IFN-γ, AACGCTACACACTGCATCTTGG (sense), GACT TCAAAGAGTCTGAGG (antisense), GGAGGAACTGGCAAAAGGA (probe). Following amplification, the DNA was analyzed by electrophoresis, Southern blotting, and hybridization with nonradioactive chemokine-specific probes. The probes were end labeled with fluorescein and identified by a chemiluminescence detection system as recommended by the manufacturer (Amersham). The chemiluminescent signals were quantified with a gel scanner calibrated with a densitometric step tablet (Kodak, Rochester, N.Y.). For each cytokine or chemokine, the results were normalized for the relative quantity of total mRNA by comparison with HPRT. Values are expressed as the fold increase or decrease of mRNA expression in organs or cultured splenocytes with respect to that of the appropriate controls, which are assigned an arbitrary value

of 1 and represent the mean and standard deviation of cytokine and chemokine mRNA levels in three individual samples for each group.

Cytotoxicity assays. The standard ^{51}Cr release assay for NK cell cytotoxicity was carried out in triplicate for each effector-to-target-cell ratio as described in detail elsewhere (24).

In vivo depletion of NK cells. Purified rabbit anti-asialo-GM_1 (as-GM_1), a polyclonal antibody (Ab) (Wako Pure Chemical Industries, Osaka, Japan), was used to deplete as-GM_1^+ (NK) cells in vivo as described previously (24). The Ab, obtained as a lyophilized preparation, was reconstituted in 1 ml of sterile distilled water and further diluted fivefold in phosphate-buffered saline prior to use. Groups of mice were given 200 μl of as-GM_1 intraperitoneally (i.p.) on days −1, 1, and 3. The mice were infected with 10^6 PFU of virus on day 0 and sacrificed on day 5.

Neutralization of IFN-γ and IFN-α/β in vivo. IFN-γ was neutralized in vivo with a monoclonal antibody (MAb) to IFN-γ (clone XMG-6; rat IgG1). A MAb to β-galactosidase (clone GL113; rat IgG1) was used as isotype-matched control. The MAbs were prepared as ascites in pristane-primed Swiss outbred nude mice. Concentrations of MAbs were determined by a sandwich enzyme-linked immunosorbent assay. Purified rabbit polyclonal Ab to murine IFN-α/β was purchased from Lee Biomolecular Research Laboratories, Inc., San Diego, Calif. Groups of mice were given 1 mg of MAb to IFN-γ or 300 U of anti-IFN-α/β or a combination of the two Abs i.p. on days −1, 1, and 3. Control mice were given 1 mg of the anti-β-galactosidase MAb. One neutralizing unit of anti-IFN-α/β is defined as the reciprocal of the dilution of antibody which completely neutralizes 10 U of the corresponding IFN activity in vitro (25). The mice were infected with 10^6 PFU of virus on day 0 and sacrificed on day 5.

Quantitation of IFNs. A sandwich enzyme-linked immunosorbent assay (28) was used to measure IFN-γ levels in culture supernatants of splenocytes (2.5×10^6) from VV-HA-TK-, VV-HA-Mig- or VV-HA–Crg-2-infected mice coincubated for 48 h with lipopolysaccharide (LPS). LPS stimulation triggers NK cells to produce IFN-γ (27). The production of IFN-γ by splenocytes from uninfected or VV-HA-TK-infected mice (day 3 p.i.) which had been cocultured with rMuMig or rCrg-2 (10 ng/ml; R & D Systems, Inc.) was also measured. Recombinant MuIFN-γ (Genzyme Diagnostics, Cambridge, Mass.) served as the standard, with an assay detection limit of 3 U/ml. In parallel experiments, treated and untreated splenocytes were collected after 8 h for mRNA isolation for the detection of IFN mRNA transcripts by RT-PCR.

Determination of virus titers in organs. Ovaries, lungs and uteri were removed asceptically from groups of four mice infected with VV-HA-TK, VV-HA-Mig, or VV-HA–Crg-2 and immediately frozen in dry ice and subsequently stored at −70°C. The organs were homogenized in 1 ml of saline containing 0.5% gelatin and 1 mM HEPES (GSH), and a 100-μl aliquot of the homogenate was incubated for 30 min with 100 μl of trypsin (1 mg/ml) at 37°C. Tenfold serial dilutions were made in GSH, and 100 μl of each dilution was added to 143B cell monolayers grown in six-well cluster plates (Flow Laboratories). After incubation for 48 h at 37°C in air containing 5% CO_2, the monolayers were stained with 0.1% crystal violet in 20% ethanol for 5 min and the plaques were enumerated.

Histologic testing. Organs were removed and fixed in 10% neutral buffered formalin solution, embedded in paraffin, sectioned (5-μm-thick sections), and stained with hematoxylin and eosin.

Statistical analysis. Results are expressed as mean ± standard error of the mean (SEM), and a two-tailed Student t test was used to determine the significance of differences between groups.

RESULTS

Protein and mRNA expression by rVVs. PCR analysis was used to confirm the presence of the genes for MuMig and Crg-2 in the F region of the appropriate rVV. It was also used to establish the absence of the parent virus, VV-HA-PR8. Amplification of DNA from VV-HA-Mig and VV-HA–Crg-2 by using the F region primers yielded the expected products of 3 and 2.8 kb, respectively (Fig. 1B, panel b). PCR analysis of VV-HA-TK DNA yielded a 1.8-kb band, the expected size in the absence of any inserts (Fig. 1B, panel a).

To demonstrate that the chemokine encoding rVV expressed MuMig or Crg-2, we analyzed concentrated supernatants that were collected from CV-1 cells infected with VV-HA-Mig, VV-HA–Crg-2, or VV-HA-TK. As shown in Fig. 2A, the recombinant viruses VV-HA-Mig and VV-HA–Crg-2 expressed the proteins MuMig and Crg-2. Due to N-linked glycosylation, carboxy-terminal processing, and probably anomalous behaviour of the polypeptide on SDS gels, MuMig runs as multiple species between 14 and 18 kDa, consistent with our previous finding (3). On the other hand, Crg-2 is not glycosylated and appears as a single species of approximately 8.7 kDa.
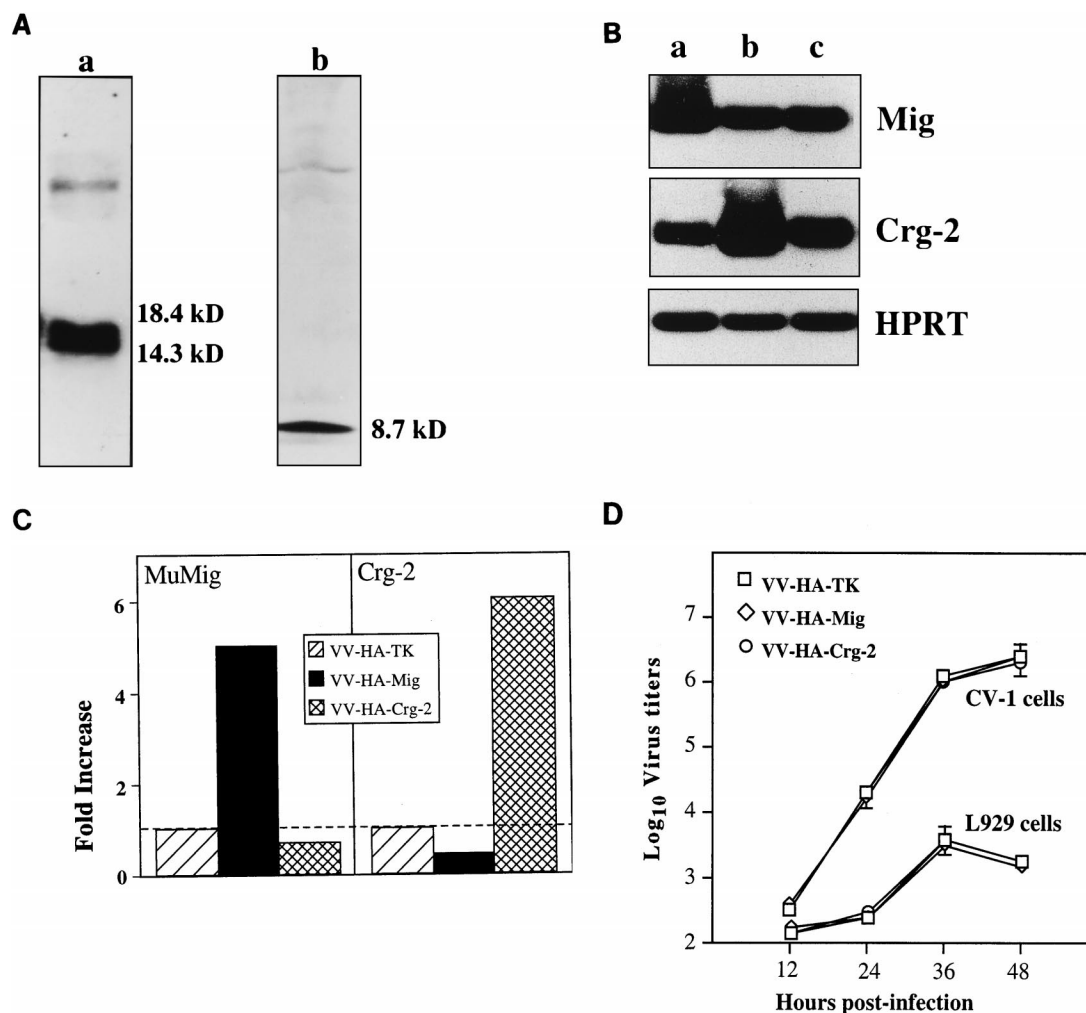
FIG. 2. (A) Production of MuMig and Crg-2 protein by rVVs. Confluent CV-1 cells were infected with VV-HA-Mig or VV-HA–Crg-2 at a multiplicity of infection of 0.1. Supernatants were collected 24 h later, protease inhibitors were added, and the samples were concentrated. Mig and Crg-2 proteins were analyzed by SDS-polyacrylamide gel electrophoresis followed by immunoblotting with anti-MuMig serum JH48 and anti-Crg-2 serum JH38, respectively. MuMig (lane a) runs as multiple species between 14 and 18 kDa, whereas Crg-2 (lane b) appears as a single species of approximately 8.7 kDa. (B) Detection of MuMig and Crg-2 mRNA in vivo by RT-PCR. Two days after infection with 10^6 PFU of VV-HA-Mig (lane a), VV-HA–Crg-2 (lane b), or VV-HA-TK (lane c), ovaries were pooled from groups of nude mice and RNA was extracted. An RT-PCR was performed for the specific genes. PCR products were electrophoresed and subjected to Southern hybridization with oligonucleotide probes and the ECL technique. The housekeeping gene, *HPRT*, was used as a control gene. (C) Quantitation of MuMig and Crg-2 mRNA transcripts in the ovaries. Values are expressed relative to VV-HA-TK-infected mice, which was assigned an arbitrary value of 1. (D) Replication of VV-HA-TK, VV-HA–Mig, and VV-HA–Crg-2 in CV-1 and L929 cells. Data shown are means ± SEM from triplicate cultures for each time point.

To further establish that rVV-encoded chemokines were expressed in vivo following infection, we examined the expression of MuMig and Crg-2 mRNA transcripts in ovaries 2 days after infection of nude mice with 10^6 PFU of virus. We chose the ovaries because VV replicates to high titers in these organs (23, 24). Figure 2B and C show increased levels of MuMig (fivefold) and Crg-2 (sixfold) mRNA expression in ovaries of nude mice infected with VV-HA-Mig or VV-HA-Crg-2, respectively, compared with expression in mice infected with the control VV-HA-TK. The chemokine mRNA levels were increased despite the 10- to 100-fold-lower VV-HA-Mig and VV-HA–Crg-2 titers compared to those of VV-HA-TK at this time (see below).

Kinetics of rVV replication in vitro. We assessed the growth characteristics of the control and chemokine-encoding rVVs in vitro by using CV-1 and L929 cells. At 12, 24, 36, and 48 h p.i., VV-HA-TK, VV-HA-Mig and VV-HA–Crg-2 replicated to comparable levels (Fig. 2D). Thus, insertion of MuMig or Crg-2 in the F region of the VV genome did not alter the capacity of the rVVs to replicate in vitro.

Mortality in athymic Swiss outbred nude mice. The effects of virus-expressed MuMig and Crg-2 on the survival of nude mice were determined. Groups of female outbred nude mice were injected intravenously (i.v.) with different doses of the rVV and observed for 60 days. At all doses tested, mice infected with the control virus VV-HA-TK experienced generalized infection and died (Table 1). The mean time to death (MTD) in mice given VV-HA-TK was dose dependent. In contrast, mice infected with 10^4 or 10^5 PFU of VV-HA-Mig or VV-HA–Crg-2 successfully resolved the infection, and no morbidity was recorded. At higher doses, however, mice infected with the rVV-encoding chemokines succumbed to disease but the MTD was significantly delayed compared to that of mice infected with comparable doses of the control virus. Mice infected with 10^6 PFU of VV-HA-TK exhibited rapid weight loss and morbidity and developed severe pox lesions on the skin by day 10 p.i. Mice infected with comparable doses of VV-HA–Crg-2 or VV-HA-Mig developed a similar condition but only after 20 days p.i. (data not shown).

TABLE 1. Effect of rVV infection on the survival of
athymic Swiss outbred nude mice[a]

Virus	MTD $\pm$ SEM following infection with virus at dose (PFU) of[b]:			
	10^7	10^6	10^5	10^4
VV-HA-TK	5.5 ± 0.5	16.8 ± 2.0	22.7 ± 4.5	35.5 ± 8.3
VV-HA-Mig	16.5 ± 2.3^d	35.2 ± 0.9^d	NM[c]	NM
VV-HA-Crg2	10.5 ± 1.0^d	29.5 ± 1.0^d	NM	NM

[a] Groups of five mice were inoculated with the indicated virus dose and observed for 60 days.
[b] Data from five individual mice.
[c] NM, no mortality.
[d] Significant ($P < 0.001$, Student's t test) compared to MTD for mice inoculated with a comparable dose of VV-HA-TK.

Kinetics of rVV replication in organs of nude mice. To determine the mechanism(s) involved in the survival of mice infected with lower doses (10^4 or 10^5 PFU) and the delayed mortality of mice given higher doses (10^6 or 10^7 PFU) of the chemokine-encoding rVV, we first determined the kinetics of virus replication and clearance in the organs of these mice. Infection with 10^5 or 10^6 PFU of VV-HA-Mig or VV-HA–Crg-2 resulted in viral titers that were significantly lower in the ovaries, uteri, and lungs than were the titers of VV-HA-TK in these organs at all time points (Fig. 3). Virus infectivity was not

detected from day 15 onward in organs of nude mice infected with 10^5 PFU VV-HA-Mig (Fig. 3A). However in organs of mice infected with 10^6 PFU, VV-HA-Mig persisted at day 15 (Fig. 3B) and thereafter (data not shown). There were no differences in VV-HA-Mig and VV-HA–Crg-2 titers in the uteri and lungs, but in the ovaries, VV-HA-Crg-2 titers were significantly higher than VV-HA-Mig titers over the entire course of infection (Fig. 3).

Splenic NK-cell activity in nude mice infected with rVV. IP-10 exhibits chemotactic activity toward NK cells and T lymphocytes in vitro (36, 55, 56), while HuMig is chemotactic for activated T lymphocytes (32). HuMig and IP-10 cause calcium fluxes in peripheral blood leukocyte-derived NK cells (35, 41). The two chemokines also have the same receptor, CXCR3, on the surface of these leukocyte subsets (33). In addition, recombinant IP-10 enhances the cytolytic activity of human NK cells in vitro (53). There was a possibility that augmented NK cell cytolytic activity due to virus-expressed Crg-2 or MuMig allowed the resolution of infection and survival of T-cell-deficient nude mice. We therefore measured splenic NK-cell activity in groups of mice inoculated with VV-HA-Mig, VV-HA–Crg-2, or the control VV-HA-TK on days 1, 2, and 3 p.i. Infection with each of these rVVs induced NK-cell cytolytic activity over and above that of uninfected controls, and activity reached a peak levels on day 3 p.i. The levels of lysis of ^{51}Cr-labeled YAC-1 targets by splenocytes obtained from mice

A. 10^5 PFU Virus
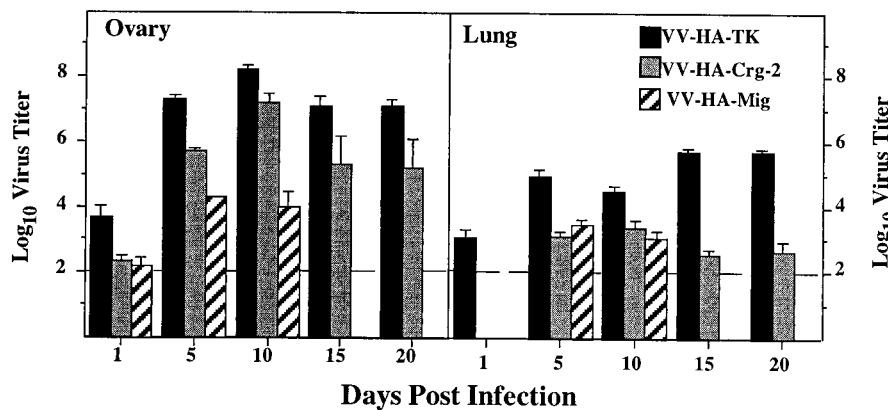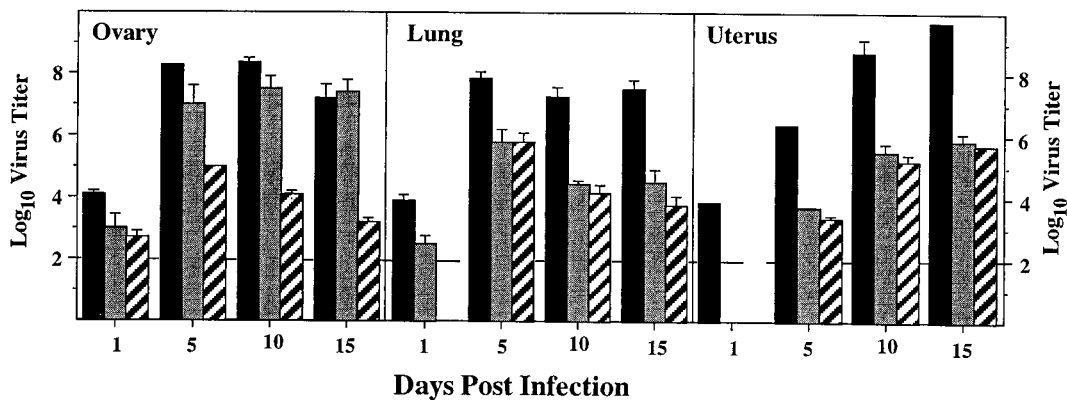

B. 10^6 PFU Virus

FIG. 3. Kinetics of rVV replication in the ovaries and lungs of outbred nude mice. Female nude mice between the ages of 6 and 9 weeks were infected intravenously with 10^5 PFU (A) or 10^6 PFU (B) of VV-HA-TK, VV-HA-Mig, or VV-HA–Crg-2, and organs were removed on the days indicated to determine virus titers. Data shown are the geometric means of four individual organs per day for each group $\pm$ SEM.
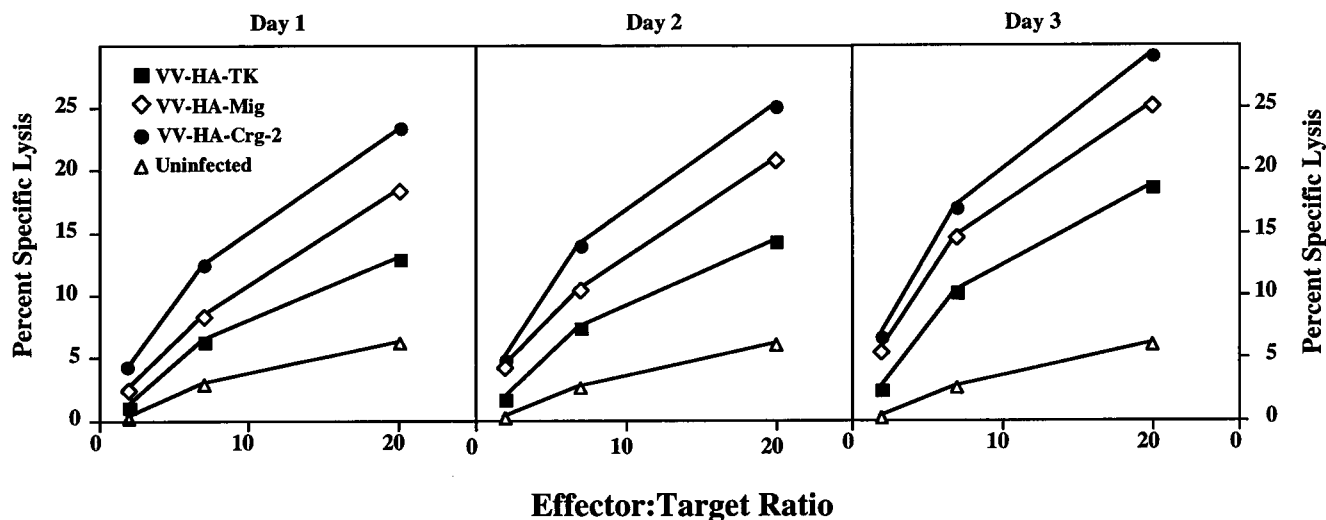
FIG. 4. Lysis of YAC-1 targets by splenocytes from athymic nude mice. NK activity was measured on days 1, 2, and 3 p.i. by using spleen cells from mice infected with 10^6 PFU of VV-HA-Mig, VV-HA–Crg-2, or VV-HA-TK. Spleen cells from uninfected mice were used as controls. Data shown are means of lysis values from four individual mice for each group. SEMs were less than 5% and have been omitted for clarity.

infected with the chemokine-encoding viruses were clearly two- to threefold higher than those obtained from control virus-infected mice (Fig. 4). In particular, the expression of virus-encoded Crg-2 enhanced NK-cell-mediated killing activity by at least threefold on each of the days tested. The increased cytolytic activity induced by virus-expressed chemokines was also accompanied by a two- to threefold increase in splenocyte numbers between days 2 and 3 p.i.

Effect of NK cell depletion on rVV replication in nude mice. Virus-expressed MuMig and particularly Crg-2 enhanced the cytolytic activity of NK cells in vivo (Fig. 4). To establish whether NK cells (as-GM$_1^+$) indeed contributed to the control of replication of the chemokine-encoding rVV, nude mice were treated with a polyclonal Ab to as-GM$_1$ to eliminate NK cells whereas control mice were left untreated. Groups of Ab-treated and untreated mice were infected i.v. with VV-HA-Mig, VV-HA–Crg-2, or VV-HA-TK and sacrificed 5 days later for the determination of virus titers.

VV-HA-TK replication was virtually unaffected whether or not NK cells had been depleted by treatment with anti-as-GM$_1$ (Table 2). In contrast, titers of VV-HA-Mig and VV-HA–Crg-2 in both ovaries and lungs increased by nearly 1.0 log$_{10}$ PFU in NK-cell-depleted mice compared to those in organs of untreated mice. Furthermore, titers of the chemokine-encoding viruses in the lungs of NK-cell-depleted mice were increased significantly and were no different from VV-HA-TK infectivity levels in this organ. Similarly, in the ovaries of NK-cell-depleted mice, VV-HA-Crg-2 titers were comparable to those of VV-HA-TK in both Ab-treated and untreated mice. Nonetheless, VV-HA-Mig titers never reached the levels of the other two rVV even in the absence of NK cells. These results clearly indicate that as-GM$_1^+$ NK cells are important for control of the chemokine-encoding viruses in the lungs but that another mechanism(s), in addition to NK-cell-mediated cytolysis, may be involved in VV-HA-Mig clearance in the ovaries. They also raise the possibility that MuMig is more potent than Crg-2 or that the as-GM1$^+$ cells may not be fully effective in the ovaries against VV-HA-Mig.

Effect of IFN depletion on rVV replication in nude mice. The results of the preceding experiments suggested that NK cells and probably another effector mechanism(s) contributed to control of the chemokine-encoding rVV in nude mice. There

was a distinct possibility that virus-encoded chemokines controlled virus replication in synergy with host-derived IFN-α/β and/or IFN-γ, which helped in the resolution of infection. A combined effect of augmented NK-cell cytolytic activity and IFN production by these cells could have contributed to virus clearance. We tested this possibility by treating rVV-infected mice with neutralizing Abs to IFN-γ, IFN-α/β, or a combination of the two and determined virus titers in ovaries and lungs 5 days p.i. In both these organs, titers of the control virus VV-HA-TK were only marginally affected following treatment with Ab to either IFN-γ or IFN-α/β (Table 3). Neutralization of both IFN-α/β and IFN-γ had no influence on virus growth in the ovaries, but viral titers in the lungs were increased by 1.0 log$_{10}$ PFU. In contrast, titers of VV-HA–Crg-2 and VV-HA-Mig in the ovaries and lungs of mice treated with antibodies to either IFN were increased by between 0.5 and 1.0 log$_{10}$ PFU above those in untreated controls. However, the most dramatic effects were seen when Abs to both IFN-α/β and IFN-γ were given simultaneously to mice infected with the chemokine-encoding rVV. Titers of VV-HA–Crg-2 and VV-HA-Mig were increased between 1.5 and 2.5 log$_{10}$ PFU and were comparable

TABLE 2. Effect of anti-as-GM$_1$ Ab treatment on rVV replication in nude mice

Virus infection and treatment[a]	Log$_{10}$ mean virus titers ± SEM[b] in:	
	Ovaries	Lungs
VV-HA-TK	8.1 ± 0.1	5.1 ± 0.3
VV-HA-TK + anti-as-GM$_1$	8.3 ± 0.4	5.2 ± 0.5
VV-HA–Crg-2	7.0 ± 0.4	4.3 ± 0.2
VV-HA–Crg-2 + anti-as-GM$_1$	8.0 ± 0.2[c]	5.3 ± 0.3[d]
VV-HA-Mig	5.0 ± 0.2	4.0 ± 0.1
VV-HA-Mig + anti-as-GM$_1$	5.9 ± 0.4[c]	4.9 ± 0.2[e]

[a] Female outbred nude mice, 6 to 9 weeks old, were given Ab to as-GM$_1$ i.p. on days −1, 1, and 3. Untreated mice infected with recombinant virus were used as controls. Mice were infected i.v. with 10^6 PFU virus on day 0, and 5 days later the mice were killed and the virus titers in their organs were determined.
[b] Data shown are the geometric means of organ titers from four mice ± SEM.
[c] $P < 0.05$ compared to viral titers in control Ab-treated mice.
[d] $P < 0.01$ compared to viral titers in control Ab-treated mice.
[e] $P < 0.005$ compared to viral titers in control Ab-treated mice.

TABLE 3. Effect of treatment with Ab to IFN-γ or IFN-α/β or both on rVV replication in nude mice

rVV infection and treatment[a]	Log10 mean virus titers ± SEM[b] in:	
	Ovaries	Lungs
VV-HA-TK		
+GL113	8.0 ± 0.2	5.1 ± 0.3
+anti-IFN-α/β	8.2 ± 0.5	5.4 ± 0.3
+anti-IFN-γ	8.2 ± 0.1	5.4 ± 0.3
+anti-IFN-α/β + anti-IFN-γ	8.3 ± 0.4	6.0 ± 0.2[c]
VV-HA-Crg-2		
+GL113	6.4 ± 0.2	4.1 ± 0.1
+anti-IFN-α/β	7.4 ± 0.2[d]	5.0 ± 0.1[d]
+anti-IFN-γ	7.4 ± 0.2[d]	5.1 ± 0.3[c]
+anti-IFN-α/β + anti-IFN-γ	8.1 ± 0.1[d]	6.1 ± 0.4[d]
VV-HA-Mig		
+GL113	5.0 ± 0.3	4.0 ± 0.1
+anti-IFN-α/β	5.5 ± 0.2	4.7 ± 0.3[c]
+anti-IFN-γ	5.8 ± 0.1[c]	4.9 ± 0.2[d]
+anti-IFN-α/β + anti-IFN-γ	7.5 ± 0.3[d]	5.4 ± 0.2[d]

[a] Groups of 6- to 9-week-old female outbred nude mice were given MAb to IFN-γ or 300 U of anti IFN-α/β or both antibodies. Mice treated with MAb GL113 were used as controls. The mice were infected i.v. with 10^6 PFU of virus on day 0 and sacrificed 5 days later for determination of virus titers in organs. These experiments were repeated twice, with reproducible results.
[b] As described for Table 2.
[c] $P < 0.05$ compared to viral titers in control Ab-treated mice.
[d] $P < 0.005$ compared to viral titers in control Ab-treated mice.

to titers in the organs of mice infected with the control VV-HA-TK and treated with these Abs. These results indicate that clearance of VV-HA-Mig and VV-HA–Crg-2 is dependent on host-derived IFNs.

IFN expression in spleens of mice infected with rVV. Efficient clearance of VV-HA-Mig and VV-HA–Crg-2 clearly required IFNs. It is possible that virus-expressed chemokines mediated rVV clearance in synergy with host-derived IFNs and/or induced the secretion of these factors. To determine whether MuMig and Crg-2 triggered the secretion of IFNs in nude mice, splenocytes (2×10^6) from mice infected with rVV (day 3 p.i.) were cultured in vitro in the presence of 10 μg of LPS per ml. In parallel, splenocytes from uninfected or VV-HA-TK-infected mice (day 2 p.i.) were cultured in the presence of 10 ng of recombinant MuMig or Crg-2 protein per nl. Untreated splenocytes were used as controls. Culture supernatants were collected after 48 h for quantitation of IFN-γ. In some experiments, splenocytes were collected after 8 hr for mRNA isolation for the detection of IFN mRNA transcripts by RT-PCR.

There were no differences in the levels of IFN-γ protein in culture supernatants of splenocytes obtained from mice infected with the chemokine-encoding viruses compared with those from control virus-infected mice (Fig. 5A). Additionally, incubation of splenocytes from nude mice with rMuMig or rCrg-2 did not induce IFN-γ production (data not shown). However, mRNA transcripts for IFN-α, IFN-β, and IFN-γ were about 1.5- to 2-fold higher in splenocytes of mice infected with the chemokine-encoding rVV compared to splenocytes of VV-HA-TK-infected mice (Fig. 5B). Such an increase was not evident in the splenocyte cultures treated with recombinant chemokines (data not shown). It is possible that increases in the levels of mRNA transcripts for IFNs in spleens of mice infected with VV-HA-Mig or VV-HA–Crg-2 are related to the increases in splenic cellularity. These results suggested that the chemokine-encoding viruses may have contributed to virus

clearance in synergy with host-derived IFNs in nude mice and not through up-regulation of their production.

Histological analysis of ovaries and livers of nude mice infected with rVV. Histological examination of ovaries 5 days after infection with 10^6 PFU of VV-HA-TK revealed extensive damage to the stromal tissue and follicles, but damage caused by VV-HA–Crg-2 infection was not as severe and minimal histopathological changes were evident in ovarian sections of VV-HA-Mig infected mice (Fig. 6). Interestingly, throughout the course of infection with VV-HA-Mig, no pathologic changes were observed in the ovaries of these mice (data not shown). The histological changes were clearly consistent with the reduced levels of rVV replication in this organ. In the liver, mononuclear cell infiltration was more prominent 2 days after infection with VV-HA–Crg-2 and VV-HA-Mig than after infection with VV-HA-TK (Fig. 7). This was despite the reduced levels of replication of the chemokine-encoding viruses in this organ (VV-HA-TK = 3.9 ± 0.2 $\log_{10}$ PFU; VV-HA-Mig = 2.0 ± 0.1 $\log_{10}$ PFU; VV-HA-Crg-2 = 2.4 ± 0.2 $\log_{10}$ PFU). Furthermore, mononuclear cell infiltration was more prominent in livers of mice infected with VV-HA–Crg-2 than in livers of mice infected with VV-HA-Mig. While this may be consistent with the slightly reduced levels of VV-HA-Mig infectivity compared to VV-HA–Crg-2 in the liver, it may also be a reflection of the differential chemoattractant properties of the two chemokines.

DISCUSSION

The IFNs are essential components of nonspecific antiviral defense mechanisms. They are important for the control of
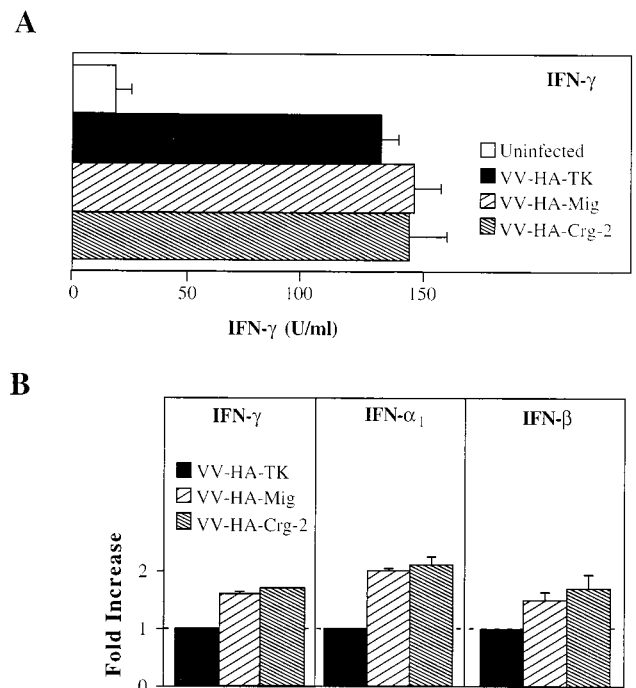
A

B

FIG. 5. (A) Splenocytes (2.5×10^6) were prepared from rVV-infected mice 3 days after infection. Splenocytes from uninfected mice were used as controls. Following stimulation with LPS for 48 h, culture supernatants were harvested and quantitated for IFN-γ by enzyme-linked immunosorbent assay. (B) Splenocytes prepared as in panel A were harvested 8 h after stimulation with LPS, and total RNA was isolated. RT-PCR analysis was performed with specific primer pairs for IFN-α1, IFN-β, and IFN-γ. Values are expressed relative to mRNA levels in splenocytes from VV-HA-TK-infected mice, which were assigned an arbitrary value of 1.
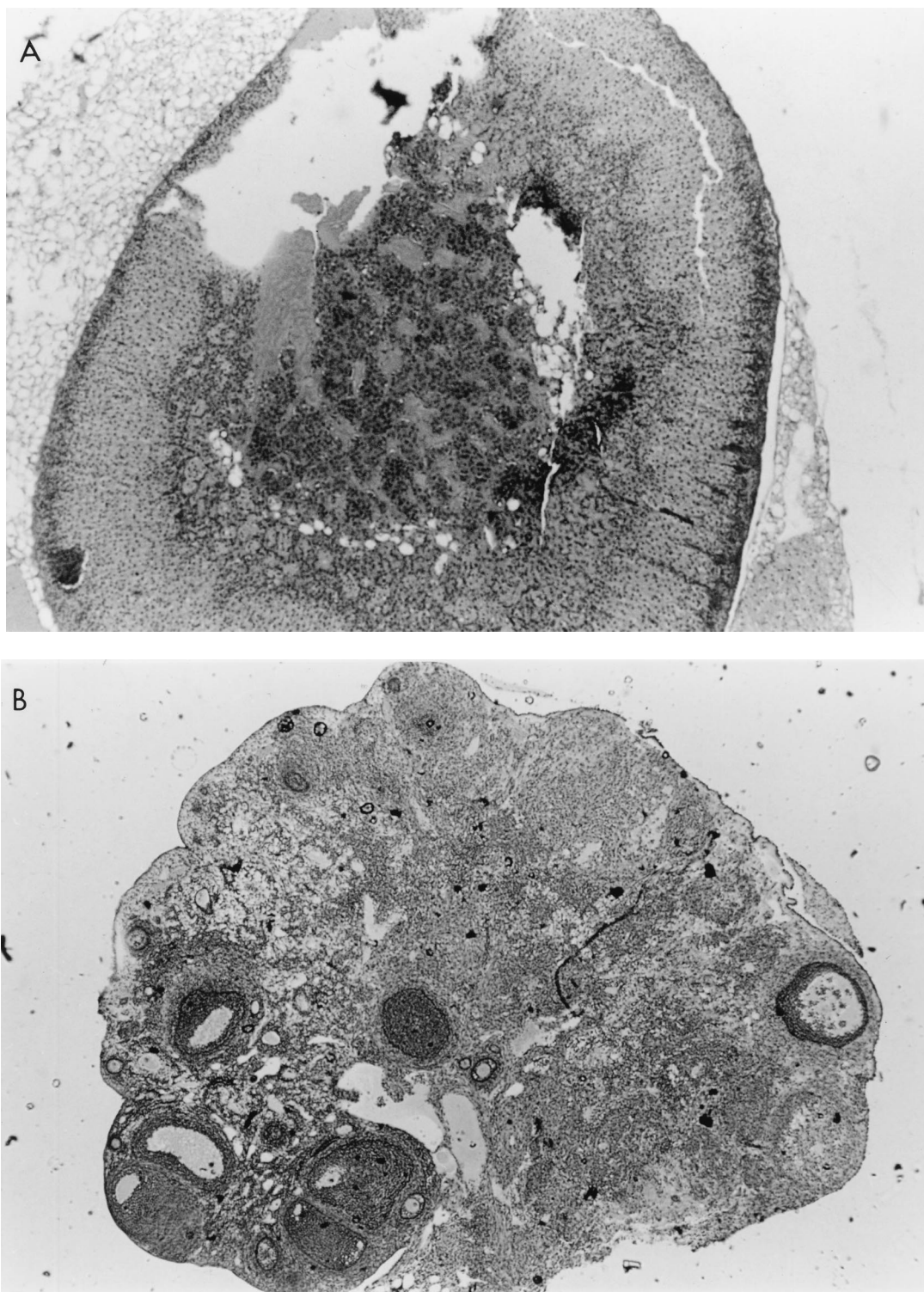
FIG. 6. Histological changes in the ovaries of nude mice infected with rVV. Hematoxylin-and-eosin-stained histological sections of ovaries taken from nude mice 5 days after infection with 10^6 PFU of VV-HA-TK, VV-HA-Mig, or VV-HA–Crg-2 are shown. (A) The rapid replication of VV-HA-TK to high titers in ovaries caused massive destruction of the ovarian stromal cells. (B and C) Partial destruction was observed in ovaries of mice infected with VV-HA–Crg-2 (B), and minimal destruction was observed in ovaries of mice infected with VV-HA-Mig (C). (D) A histological section from an uninfected control mouse is also shown. Magnification, ×100.

virus replication and spread before virus-specific immune responses such as cytotoxic T lymphocytes and antibody are generated. Experimental mice rendered deficient for the production of IFN-γ (11) or IFN receptors (22, 38) or treated with neutralizing Ab to IFNs (23, 25) are highly susceptible to infection with poxviruses despite the generation of virus-specific immune responses.

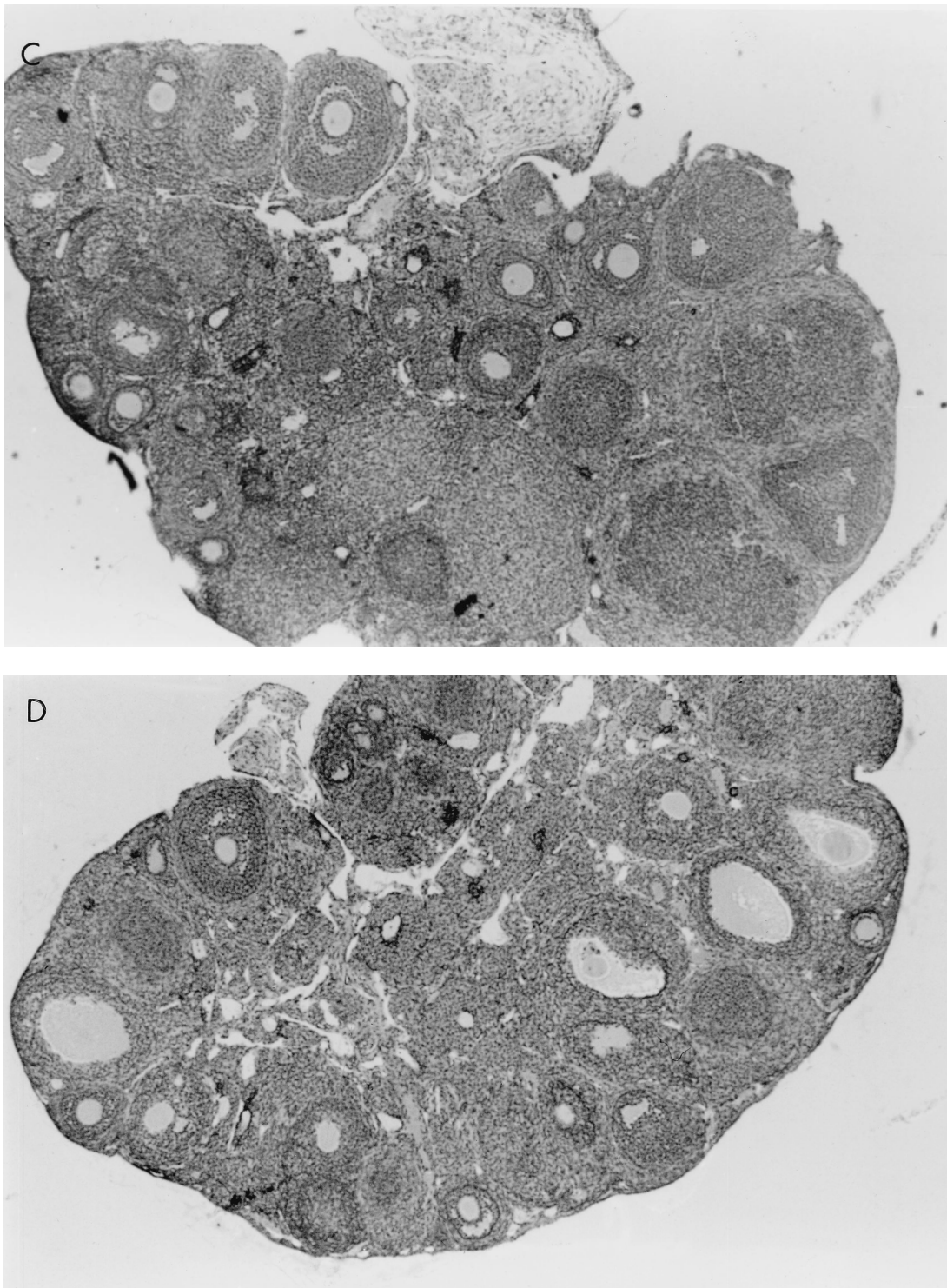The antiviral activity of IFNs is mediated through induction

FIG. 6—*Continued.*

of several other proteins and enzymes as well as through activation of NK cells (26, 48). It is known that Mig and Crg-2/IP-10 are both IFN-inducible proteins. IP-10 exhibits chemotactic activity towards NK cells in addition to enhancing the cytolytic activity of this leukocyte subset in vitro (35, 52, 53). Additionally, IP-10 and HuMig can cause calcium fluxes in PBL-derived NK cells (35, 42). The two chemokines also have the same receptor, CXCR3, on the surface of NK cells (33). These findings led us to speculate that Mig and Crg-2 may, in fact, mediate some of the antiviral effects of IFNs. In this study, we used the rVV encoding MuMig or Crg-2 in combination with the nude-mouse model to study the effects of these IFN-inducible chemokines in vivo.

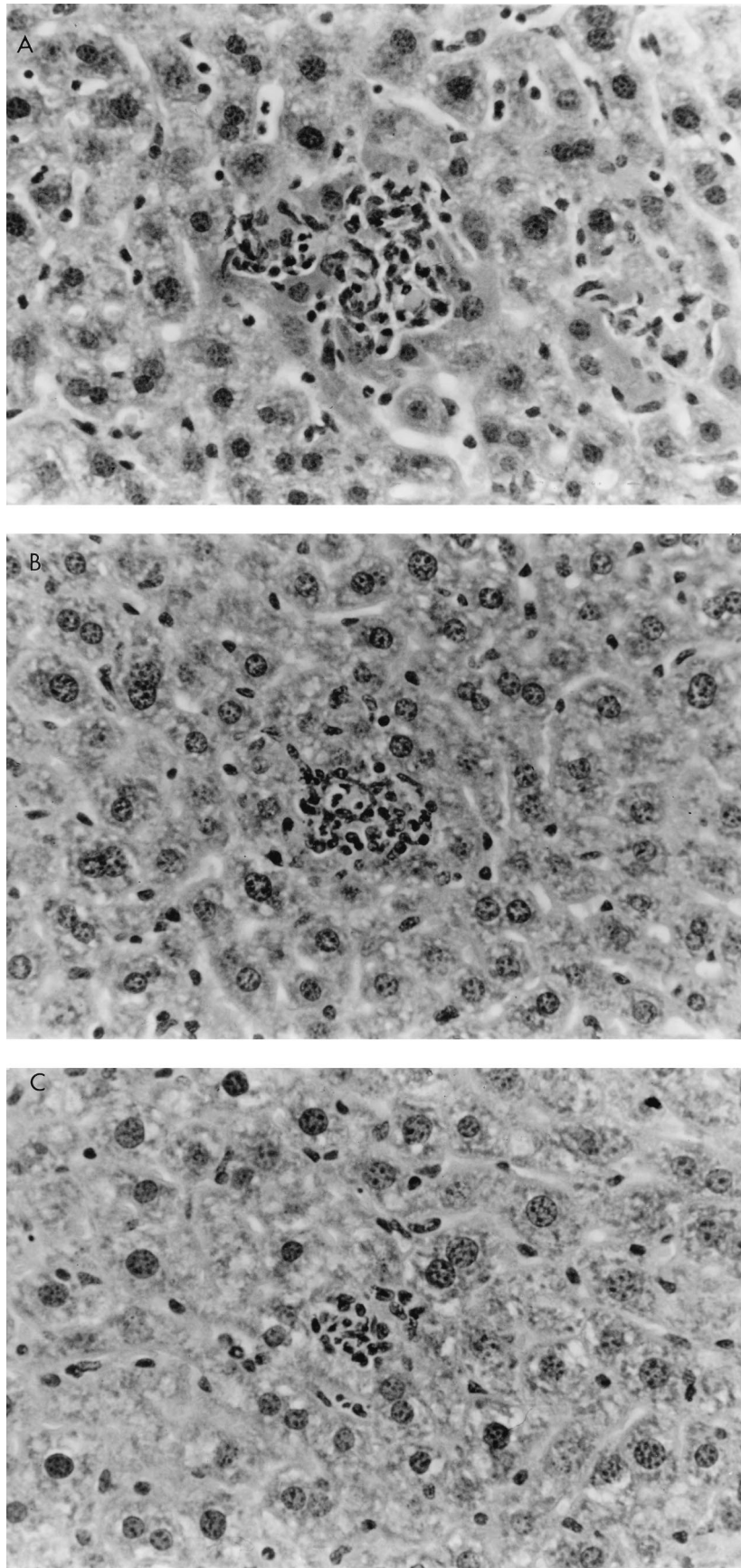The control virus (VV-HA-TK) proved lethal for nude mice

FIG. 7. Hematoxylin-and-eosin-stained histological sections of livers from nude mice 48 h after i.v. injection with 10^6 PFU of rVV. Increased mononuclear cell infiltration was typically seen in liver lesions caused by VV-HA–Crg-2 (A) and VV-HA-Mig (B) with respect to that seen in lesions caused by VV-HA-TK (C). Magnification, ×150.

at all doses tested, consistent with earlier findings (29, 42, 43). In contrast, the expression of MuMig or Crg-2 during infection with lower doses (10^4 to 10^5 PFU) of rVV resulted in marked attenuation and reduced pathogenicity, with 100% survival of nude mice. Increased doses of these viruses ($\geq 10^6$ PFU) were nevertheless lethal, but the MTD was significantly longer than that of mice given comparable doses of the control rVV (Table 1). Clearly, while the chemokine-induced antiviral mechanism(s) was effective for the control of low-dose rVV infection, it was insufficient to clear virus at higher doses. This contrasts with clearance of rVV encoding the type 1 cytokines IL-2, IFN-γ, or TNF in nude mice (43). The T-cell-deficient animals were able to clear each of these rVVs when inoculated with as much as 10^7 PFU. Virus-expressed IFN-γ or TNF apparently exhibited direct antiviral activity, whereas rVV encoding IL-2 augmented the cytolytic activity of NK cells and induced the synthesis of IFN-γ by these as well as other leukocyte populations (23, 24). In the present study, the capacity of nude mice to resolve a low-dose infection with either of these chemokine-encoding rVVs was clearly related to levels of replication, with each being recovered at significantly lower titers than the control virus in all organs at all times (Fig. 3).

The finding that receptors for Mig and IP-10/Crg-2 are expressed on the surface of NK cells (33) suggests that Mig and Crg-2 may be important both in the recruitment of NK cells to the site of infection and in their activation which may involve enhancement of the lytic activity. Indeed, recombinant IP-10 enhances the cytolytic activity of human NK cells in vitro (35, 53). At least two lines of evidence indicate that virus-expressed MuMig and Crg-2 influenced the antiviral activity of NK cells in vivo. First, the cytolytic activity of splenic NK cells obtained from the chemokine-encoding rVV-infected mice was at least two- to threefold higher than that of the control VV-HA-TK-infected mice. Whether this increase in killing activity is on a per-cell basis is not clear, but it may be related to the two- to threefold increase in splenic cellularity (see below). Second, elimination of NK cells (as-GM$_1$$^+$ cells) with antibody exacerbated infection with the chemokine-encoding viruses but had a negligible effect on the replication of the control virus. These findings established a definitive role for NK cells in the control of the chemokine-encoding rVV replication in nude mice.

For NK cells to operate against viral infection in vivo, they have to be present at foci of infection. This allows their cytolytic activity as well as the soluble mediators they produce (see below) to prevent further virus replication in infected cells and to protect uninfected cells, respectively. Examination of histological sections revealed increased numbers of mononuclear cell infiltration (beginning 2 to 3 days p.i.) in livers of VV-HA–Crg-2- and VV-HA-Mig-infected mice compared to livers of control virus-infected mice. At this time, a concomitant two- to threefold increase in splenocyte numbers was evident in the former groups compared to the latter. Whether this increase in splenocyte numbers is due to proliferation is not clear, but a combined effect of increased cell numbers in infectious foci and augmented killing activity could have contributed to control of virus replication. Indeed, it has been shown that NK cells migrate to the red pulp/white pulp border in the spleen following viral infections (44). In addition, some of us have recently demonstrated that MuMig and Crg-2 are expressed in CD11b$^+$ cells, presumably macrophages, at the margin between the red and white pulps in the spleen (3). Given that both MuMig and Crg-2 are chemotactic for NK cells, it is possible that a proportion of these infiltrating cells are of this phenotype. Histological analysis of livers of nude mice treated with Ab against as-GM$_1$$^+$ (NK) cells and infected with the chemokine-encoding viruses displayed a reduction in cellular

infiltrate compared to untreated infected mice (37). Our findings, as well as those of others, suggest that there may be a causal relationship between expression of these chemokines and NK cell localization at this site (3, 37, 45). Since immunostaining of spleen sections from nude mice with anti-as-GM$_1$ has been unsuccessful, we are currently investigating the phenotype of the infiltrating cells in euthymic mice infected with chemokine-encoding rVV. Infection of euthymic C57BL/6 mice results in rapid clearance of the chemokine-encoding rVV, with a similar increase in the mononuclear cell infiltration in the liver (37).

In athymic nude mice, NK cells and to a lesser extent γδ-TCR$^+$ T cells produce IFN-γ (23, 40, 55) whereas these and other cell types produce IFN-α/β. Thus, increases in cell numbers (NK cells and other leukocyte populations) in infectious foci would also lead to increased production of IFNs locally. These antiviral factors are critical for recovery from VV infection. For these reasons, we examined the role of IFNs in the control of the chemokine-encoding rVV by using specific neutralizing Abs. Indeed, treatment with anti-IFN-α/β or anti-IFN-γ significantly increased VV-HA-Mig and VV-HA–Crg-2 titers but not those of the control virus. Neutralization of both IFN-α/β and IFN-γ simultaneously completely abolished the chemokine-mediated antiviral effects, since the titers were no different from those of the control virus. These data indicate two pertinent points. First, rVV-encoded MuMig and Crg-2 mediate antiviral activity in vivo and this process is dependent on IFN-α, IFN-β, and IFN-γ. Second, there are no intrinsic differences in the in vivo growth characteristics of the rVV, and this is apparent only in mice with virtually no immune function. In vitro, all three rVVs replicated to comparable levels.

The amounts of IFN-γ produced by cultured splenocytes from the chemokine-encoding rVV-infected nude mice were comparable to those produced by splenocytes from control virus-infected mice (Fig. 5A). In addition, recombinant MuMig or Crg-2 did not induce nude-mouse splenocytes to secrete IFN-γ. While levels of mRNA transcripts for IFN-α, IFN-β, and IFN-γ in spleens of mice infected with the chemokine-encoding rVVs were increased by 1.5- to 2-fold over those of control rVV-infected mice, rMuMig or rCrg-2 did not induce similar increases in the levels of mRNA transcripts for IFNs in vitro. Thus, the 1.5- to 2-fold increases may be related to the increased splenic cellularity in VV-HA-Mig- or VV-HA–Crg-2-infected mice. It is possible that such increases also resulted in increased frequencies of NK cells. Thus, the antiviral effects of the chemokines MuMig and Crg-2 do not appear to be mediated through the upregulation of IFN production. Rather, a combined effect of increased NK-cell numbers with augmented cytolytic activity as well as their capacity to produce IFN in infectious foci contribute to virus clearance. This is in contrast to the mechanism(s) of rapid virus clearance by virus-expressed IL-2 (23, 24). Infection of athymic nude mice with rVV encoding IL-2 results in augmented NK-cell cytolytic activity as well as increased IFN-γ secretion on a per-cell basis. This is accompanied by increased mononuclear cell (NK- and non-NK-cell) infiltration in foci of infection. The capacity of rVV-expressed IL-2 to induce IFN-γ secretion as well as to augment NK-cell killing allowed rapid resolution of infection with high-virus dose (10^7 PFU). The inability of rVV-expressed MuMig or Crg-2 to trigger IFN-γ production could explain why infection of nude mice with higher doses of the chemokine-encoding rVV proved lethal. Mortality due to infection with higher doses of the chemokine-encoding viruses was, nevertheless, delayed significantly compared to the mortality of mice given an equivalent dose of the control rVV. Thus, in the

absence of T lymphocytes, augmented NK-cell killing alone is not sufficient to control high-dose rVV infection.

We have previously shown that VV can replicate to high titers in the ovaries, and histological analyses of this organ showed extensive inflammation and tissue destruction (24). Destruction of the ovaries of mice infected with VV-HA–Crg-2 was not severe, and ovaries of mice infected with VV-HA-Mig appeared intact, consistent with the levels of virus replication. Clearly, Mig and Crg-2 exhibited different levels of protection in the ovaries but not in the lungs or uteri. This may be a reflection of the differential chemoattractant and/or antiviral properties of the two chemokines, but this is not known. However, the differential induction of Mumig and Crg-2 in vivo in multiple organs following VV infection suggests nonredundant roles for these IFN-inducible chemokines (3).

The roles of chemokines have been studied extensively in inflammatory diseases and in models of inflammation (5, 6). Their contributions to the control of viral infections has only recently been explored. For instance, MIP-1α-deficient mice lack an inflammatory myocardial response to coxsackievirus infection (9). Similarly, infection of these mutant mice with influenza A virus results in a substantially reduced mononuclear infiltration in the lungs, but virus clearance is also significantly delayed, indicating that MIP-1α represents a major factor for the localization of mononuclear cells to the site of viral infection. Whether this chemokine exhibits direct antiviral activity against influenza A virus is not known, but recent investigations of CD8^{+}-T-cell-derived products which were found to inhibit HIV replication in vitro led to the discovery that the HIV-1-suppressive factors were indeed the CC chemokines RANTES, MIP-1α, and MIP-1β (8). This, together with the findings that the chemokine receptors CCR5 and CXCR4 act as cofactors for HIV-1, may lead to the development of new therapeutic strategies such as the use of viral vectors encoding chemokines or chemokine antagonists aimed at blocking the viral access to the receptor.

Our approach of using chemokine-encoding rVV to study the activities of MuMig and Crg-2 in vivo has clearly shown that these IFN-inducible CXC chemokines mediate antiviral activity through recruitment and activation of a distinct leukocyte subset(s) as well as optimizing IFN production at sites of virus replication.

ACKNOWLEDGMENTS

REFERENCES

1. Alcami, A., and G. L. Smith. 1995. Vaccinia, cowpox and camelpox viruses encode soluble gamma interferon receptors with novel broad species specificity. J. Virol. 69:4633–4639.
2. Alkhatib, G., C. Combadiere, C. C. Broder, Y. Feng, P. E. Kennedy, P. M. Murphy, and E. A. Berger. 1996. CC CKR5: a RANTES, MIP-1α, MIP-1β receptor as a fusion cofactor for macrophage-tropic HIV-1. Science 272:1955–1958.
3. Amichay, D., R. T. Gazzinelli, G. Karupiah, T. R. Moench, A. Sher, and J. M. Farber. 1996. The gene for chemokines MuMig and Crg-2 are induced in protozoan and viral infections in response to IFN-γ with patterns of tissue expression that suggest nonredundant roles in vivo. J. Immunol. 157:4511–4520.
4. Andrew, M. E., B. E. H. Coupar, G. L. Ada, and D. B. Boyle. 1986. Cell-mediated immune responses to influenza virus antigens expressed by vaccinia virus recombinants. Microb. Pathog. 1:443–452.
5. Bacon, K. B., and T. J. Schall. 1996. Chemokines as mediators of allergic inflammation. Int. Arch. Allergy Immunol. 109:97–109.
6. Baggiolini, M. 1998. Chemokines and leukocyte traffic. Nature 392:565–568.
7. Choe, H., M. Frazan, Y. Sun, N. Sullivan, B. Rollins, P. D. Ponath, L. Wu, C. R. Mackay, G. LaRosa, W. Newman, N. Gerard, C. Gerard, and J. Sodroski. 1996. The beta-chemokine receptors CCR3 and CCR5 facilitate infection by primary HIV-1 isolates. Cell 85:1135–1148.
8. Cocchi, F., A. L. DeVico, A. Garzino-Demo, S. K. Arya, R. C. Gallo, and P. Lusso. 1995. Identification of RANTES, MIP-1α, and MIP-β as the major HIV-suppressive factors produced by CD8^{+} T cells. Science 270:1811–1815.
9. Cook, D. N., M. A. Beck, T. M. Coffman, S. L. Kirby, J. F. Sheridan, I. B. Pragnell, and O. Smithies. 1995. Requirement of MIP-1α for an inflammatory response to viral infection. Science 269:1583–1585.
10. Coupar, B. E. H., M. E. Andrew, and D. B. Boyle. 1988. A general method for the construction of recombinant vaccinia viruses expressing multiple foreign genes. Gene 68:1–10.
11. Dalton, D. K., S. Pitts-Maek, S. Keshav, I. S. Figari, A. Bradley, and T. A. Stewart. 1993. Multiple defects of immune cell function in mice with disrupted interferon-γ genes. Science 259:1739–1742.
12. Deng, H., R. Liu, W. Ellmeier, S. Choe, D. Ynutmaz, M. Burkhart, P. Di-Marzio, S. Marmon, R. E. Sutton, C. M. Hill, C. B. Davis, S. C. Peiper, T. J. Schall, D. R. Littman, and N. R. Landau. 1996. Identification of a major co-receptor for primary isolates of HIV-1. Nature 381:661–666.
13. Doranz, B. J., J. Rucker, Y. Yi, R. J. Smyth, M. Samson, S. C. Peiper, M. Parmentier, R. G. Collman, and R. W. Doms. 1996. A dual-tropic primary HIV-1 isolate that uses fusin and the beta-chemokine receptors CKR-5, CKR-3, and CKR-2b as fusion cofactors. Cell 85:1149–1158.
14. Dragic, T., V. Litwin, G. P. Allaway, S. R. Martin, Y. Huang, K. A. Nagashima, C. Cayanan, P. J. Maddon, R. A. Koup, J. P. Moore, and W. A. Paxton. 1996. HIV-1 entry into CD4+ cells is mediated by the chemokine receptor CC-CKR5. Nature 381:667–673.
15. Farber, J. M. 1990. A macrophage mRNA selectively induced by γ-interferon encodes a member of the platelet factor 4 family of cytokines. Proc. Natl. Acad. Sci. USA 87:5238–5242.
16. Farber, J. M. 1992. A collection of mRNA species that are inducible in the RAW 264.7 mouse macrophage cell line by gamma interferon and other agents. Mol. Cell. Biol. 12:1535–1545.
17. Farber, J. M. 1993. A new human member of the chemokine family of cytokines. Biochem. Biophys. Res. Commun. 192:223–230.
18. Feng, Y., C. C. Broder, P. E. Kennedy, and E. A. Berger. 1996. HIV-1 entry cofactor: functional cDNA cloning of a seven-transmembrane, G protein-coupled receptor. Science 272:872–877.
19. Gao, J. L., and P. M. Murphy. 1994. Human cytomegalovirus open reading frame US28 encodes a functional β chemokine receptor. J. Biol. Chem. 269:28539–28542.
20. Heine, H. G., and D. B. Boyle. 1993. Infectious bursal disease virus structural protein VP2 expressed by a fowlpox virus recombinant confers protection against disease in chickens. Arch. Virol. 131:277–292.
21. Horuk, R., C. E. Chitnis, W. C. Darbonne, T. J. Colby, A. Rybicki, T. J. Hadley, and L. H. Miller. 1993. A receptor for the malarial parasite Plasmodium vivax: the erythrocyte chemokine receptor. Science 261:1182–1184.
22. Huang, S., W. Hendriks, A. Althage, S. Hemmi, H. Bluethmann, R. Kamijo, J. Vilcek, R. M. Zinkernagel, and M. Aguet. 1993. Immune response in mice that lack the interferon-γ receptor. Science 259:1742–1745.
23. Karupiah, G., R. V. Blanden, and I. A. Ramshaw. 1990. Interferon γ is involved in the recovery of athymic nude mice from recombinant vaccinia virus/interleukin 2 infection. J. Exp. Med. 172:1495–1503.
24. Karupiah, G., B. E. H. Coupar, M. E. Andrew, D. B. Boyle, S. M. Phillips, A. Mullbacher, R. V. Blanden, and I. A. Ramshaw. 1990. Elevated NK cell responses in mice infected with recombinant vaccinia virus encoding murine IL-2. J. Immunol. 144:290–298.
25. Karupiah, G., T. N. Fredrickson, K. L. Holmes, L. H. Khairallah, and M. L. Buller. 1993. Importance of interferons in recovery from mousepox. J. Virol. 67:4214–4226.
26. Karupiah, G., Q.-W. Xie, R. M. L. Buller, C. Nathan, C. Duarte, and J. D. MacMicking. 1993. Inhibition of viral replication by interferon-γ-induced nitric oxide synthase. Science 261:1445–1448.
27. Karupiah, G., T. Sacks, D. Klinman, J. Hartley, J. Chen, T. Fredrickson, and H. C. Morse III. 1998. Murine cytomegalovirus infection-induced polyclonal B-cell activation is independent of CD4+ T cells and CD40. Virology 240:12–26.
28. Karupiah, G., J.-H. Chen, C. Nathan, S. Mahalingam, and J. MacMicking. 1998. Identification of nitric oxide synthase locus 2 as an innate resistance locus against ectromelia virus infection. J. Virol. 72:7703–7706.
29. Kohonen-Corish, M. R. J., N. J. C. King, C. E. Woodhams, and I. A. Ramshaw. 1990. Immunodeficient mice recover from infection with vaccinia virus expressing interferon-γ. Eur. J. Immunol. 20:157–161.
30. Laemmli, U. K. 1970. Cleavage of structural proteins during the assembly of the head of the bacteriophage T4. Nature 227:680–685.
31. Liao, F., G. Alkhatib, K. W. Peden, G. Sharma, E. A. Berger, and J. M. Farber. 1997. STRL33, a novel chemokine receptor-like protein, functions as a fusion cofactor for both macrophage-tropic and T cell line-tropic HIV-1. J. Exp. Med. 185:2015–2023.
32. Liao, F., R. L. Rabin, J. R. Yannelli, L. G. Koniaris, P. Vanguri, and J. M. Farber. 1995. Human mig chemokine: biochemical and functional characterization. J. Exp. Med. 182:1301–1314.
33. Loetscher, M., B. Gerber, P. Loetscher, S. A. Jones, L. Piali, I. C. Lewis, M. Baggiolini, and B. Moser. 1996. Chemokine receptor specific for IP-10 and

Mig: structure, function, and expression in activated T-lymphocytes. J. Exp. Med. **184:**963–969.

34. **MacDonald, M. R., X. Y. Li, and H. W. Virgin.** 1997. Late expression of a beta chemokine homolog by murine cytomegalovirus. J. Virol. **71:**1671–1678.

35. **Maghazachi, A. A., B. S. Skalhegg, B. Rolstad, and A. Al-Aoukaty.** 1997. Interferon-inducible protein-10 and lymphotactin induce the chemotaxis and mobilization of intracellular calcium in natural killer cells through pertussis toxin-sensitive and -insensitive heterotrimeric G-proteins. FASEB J. **11:**765–774.

36. **Mahalingam, S., C. L. Tan, and G. Karupiah.** Unpublished data.

37. **Mahalingam, S., J. M. Farber, and G. Karupiah.** Unpublished data.

38. **Müller, U., U. Steinhoff, L. F. Reis, J. Pavlovic, R. M. Zinkernagel, and M. Aguet.** 1994. Functional role of type I and type II interferons in antiviral defense. Science **264:**1918–1921.

39. **Oswald, I. P., T. A. Wynn, A. Sher, and S. L. James.** 1992. Interleukin 10 inhibits macrophage microbicidal activity by blocking the endogenous production of tumor necrosis factor alpha required as a costimulatory factor for interferon gamma-induced activation. Proc. Natl. Acad. Sci. USA **89:**8676–8680.

40. **Pardoll, D. M., B. J. Fowlkes, A. M. Lew, W. L. Maloy, M. A. Weston, J. A. Bluestone, R. H. Schwartz, J. E. Cooligan, and A. M. Kruisbeek.** 1988. Thymus-dependent and thymus independent developmental pathways for peripheral T cell receptor-γδ-bearing lymphocytes. J. Immunol. **140:**4091–4096.

41. **Rabin, R., M. Park, F. Liao, R. Swafford, D. Stephany, and J. M. Farber.** Unpublished data.

42. **Ramshaw, I. A., M. E. Andrew, S. M. Phillips, D. B. Boyle, and B. Coupar.** 1987. Recovery of immunodeficient mice from vaccinia virus/IL-2 recombinant infection. Nature **329:**545–546.

43. **Ramshaw, I. A., A. Ramsay, J. Ruby, G. Ada, and G. Karupiah.** 1992. Expression of cytokines by recombinant vaccinia viruses: a model for studying cytokines in virus infections in vivo. Immunol. Rev. **127:**157–182.

44. **Ramshaw, I. A., A. J. Ramsay, G. Karupiah, M. S. Rolph, S. Mahalingam, and J. C. Ruby.** 1997. Cytokines and immunity to viral infections. Immunol. Rev. **159:**119–135.

45. **Salazar-Mather, T. P., R. Ishikawa, and C. A. Biron.** 1996. NK cell trafficking and cytokine expression in splenic compartments after IFN induction and viral infection. J. Immunol. **157:**3054–3064.

46. **Schall, T. J., K. B. Bacon, K. J. Toy, and D. V. Goeddel.** 1990. Selective attraction of monocytes and T lymphocytes of the memory phenotype by cytokine RANTES. Nature **347:**669–672.

47. **Schall, T. J., K. B. Bacon, R. D. R. Camp, J. W. Kaspari, and D. V. Goeddel.** 1993. Human macrophage inflammatory protein α (MIP-1α) and MIP-1β chemokines attract distinct populations of lymphocytes. J. Exp. Med. **177:**1821–1825.

48. **Sen, G. C., and P. Lengyel.** 1992. The interferon system. A bird's eye view of its biochemistry. J. Biol. Chem. **267:**5017–5020.

49. **Spriggs, M. K., B. H. Koller, T. Sato, P. J. Morrissey, W. C. Fanslow, O. Smithies, F. Voice, M. B. Widmer, and C. R. Maliszewski.** 1992. β2-Microglobulin⁻ CD8⁺ T-cell deficient mice survive inoculation with high doses of vaccinia virus and exhibit altered IgG responses. Proc. Natl. Acad. Sci. USA **89:**6070–6074.

50. **Svetic, A., F. D. Finkelman, Y. C. Jian, C. W. Dieffenbach, D. E. Scott, K. F. McCarthy, A. D. Steinberg, and W. C. Gause.** 1991. Cytokine gene expression after in vivo primary immunization with goat antibody to mouse IgD antibody. J. Immunol. **147:**2391–2397.

51. **Symons, J. A., A. Alcami, and G. L. Smith.** 1995. Vaccinia virus encodes a soluble type I receptor of novel structure and broad species specificity. Cell **81:**551–560.

52. **Taub, D. D., A. R. Lloyd, K. Conlon, J. M. Wang, J. R. Ortaldo, A. Harada, K. Matshushima, D. J. Kelvin, and J. J. Oppenheim.** 1993. Recombinant human interferon-inducible protein 10 is a chemoattractant for human monocytes and T lymphocytes and promotes T cell adhesion to endothelial cells. J. Exp. Med. **177:**1809–1814.

53. **Taub, D. D., T. J. Sayers, C. R. D. Carter, and J. R. Ortaldo.** 1995. α and β chemokines induce NK cell migration and enhance NK-mediated cytolysis. J. Immunol. **155:**3877–3888.

54. **Vanguri, P., and J. M. Farber.** 1990. Identification of CRG-2: an interferon-inducible mRNA predicted to encode a murine monokine. J. Biol. Chem. **265:**15049–15057.

55. **Yoshikai, Y., M. D. Reis, and T. W. Mak.** 1986. Athymic mice express a high level of functional γ-chain but greatly reduced levels of α- and β-chain T-cell receptor messages. Nature **324:**482–485.